

CHAPTER 6

STATISTICAL METHOD OF ANALYSIS

A stochastic process is replicated consistently via stochastic (Monte Carlo) simulation. The results obtained from a single sample of possibilities. To gain conclusive information on the growing process of dendrites, a large number of samples or time records, under the same filtration conditions are necessary. These then would be analysed statistically to provide the desired information.

The investigated conditions are listed in Table 5.1. The sample size used in this study was 50. The computer program for statistical analysis of the simulation results for polydisperse aerosols was modified from that developed for monodisperse aerosols by Kanoaka et al. (1981). What follows is brief explanation of the methodologies used for statistical analysis.

6.1 Average Profile of Deposited Particles

The average profile of deposited mass per unit fiber length is chosen to illustrate the angular dependence of deposited particles. The cylindrical fiber was divided angle-wise into a number of angular divisions. For simplicity, the magnitude of each angular division, $\Delta\theta$, was chosen as $\Delta\theta = d_p / (R_f + r_p)$. Divisions were made symmetrical about the front stagnation plane.

To find out how the average profile evolved against filtration time, the masses of deposited particles whose centers lie either between θ and $\theta + \Delta\theta$ or between $-\theta$ and $-(\theta + \Delta\theta)$ were added up, divided by the mass of an average particle ($d_p = d_{pm}$), and averaged over the effective fiber length and over all samples under the same filtration conditions.

The relationship between the total mass of incoming particles W_{gen} and filtration time t is as follows

$$t = \frac{W_{gen}}{c_o U_\infty \cdot 2HL R_f^2} \quad (6.1.1)$$

Here t is filtration time, W_{gen} is the total mass of incoming through the generation plane up to time t , c_o is the approaching mass concentration of polydisperse aerosols, U_∞ is the approach velocity of air flow to Kuwabara's cell, H is the dimensionless half height of the generation plane, L is the dimensionless length of the generation plane, and R_f is the actual fiber diameter. The above relation allowed the use W_{gen} in place of t .

6.2 Mass Distribution of Deposited Particles in Mesh Network

Except for the spread of dust load as a function of θ along the fiber perimeter, the previous average profile does not say much about the configuration (tallness, fatness, etc.) of an average dendrite, since the shape and height of a dendrite depends not only how many particle it contains but also on how the particles are arranged. Therefore, it is interesting to know the mass distribution with which particles are deposited in meshes around the fiber perimeter. The information will reveal the side-view configuration of an average dendrite.

To do this, a two-dimensional mesh network was constructed around the fiber cross section, as shown in Figure 6.1. The radial sides and the chord spanning the outer arc of each mesh were all made equal to dimensionless geometric mean particle diameter d_{pm} . These meshes were layered on the fiber surface and constructed symmetrically about the front stagnation plane. For convenience a deposited particle whose center falls within a mesh was counted as belong to the mesh, and the mass of the particle was totalled over the effective fiber length. Since the deposition process should on the average be symmetrical about the half plane, the masses of deposited particles in an upper-half mesh and its lower half mirror image were added up divided by the mass of an average particle ($d_p = d_{pm}$), rounded, reported in the present work.

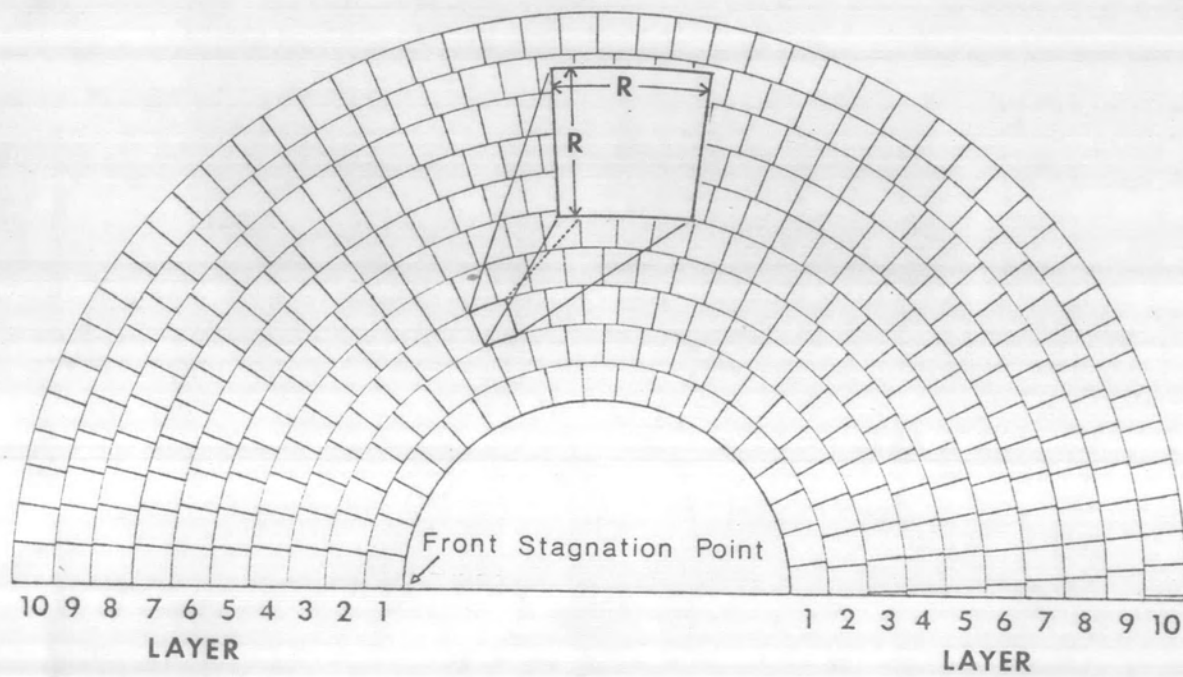


Figure 6.1 Construction of mesh network around a cylindrical fiber

6.3 Number Distribution of Dendrites versus Filtration Time

The growth of dendrites, as revealed by the total numbers of dendrites of various size existing on the effective fiber length and relevant information were collected at successive intervals of filtration time. At each interval, the number of dendrites of the same members N ($N = 1, 2, 3, \dots$) was counted, and since the deposited particles are not monosized, the total mass of dendrites of the same members N was also computed, along with the total number, equivalent number and mass of incoming particles, the weight percent and number percent of dendrites of the same members N , the total number of dendrite of all members and the total number of deposited particles.

To save space and time, only the number distribution of dendrites of the same N members ($N = 1, 2, 3, \dots$) is presented graphically as a function of equivalent number of incoming particles in Chapter 7.

6.4 Dendritic Age

The age of a dendrite is the time that has elapsed since the first number particle deposits on the fiber surface. Obviously, dendrites of the same members N do not necessarily have the same age. For the sake of convenience, when dendrites of different ages become linked or intermeshed, the age of resulting dendrite was taken to be that of the older. Obviously, only single-particle dendrites existed at birth (zero age) since aerosol particles were introduced consecutively one by one in to the system.

6.5 Number Distribution of Dendrites versus Age

As in Section 6.3, the number distribution of dendrites of the same members N ($N = 1, 2, 3, \dots$) and other related information were collected and only the number distribution of dendrites of the same members N is showed graphically as a function dendritic age in Chapter 7.

6.6 Single-Fiber Collection Efficiency under Dust Loaded Conditions

The collection efficiency of a single fiber under dust loaded conditions was also evaluated and is shown in Chapter 7. Generally the collection efficiency of a single fiber η_{DIM} is defined as the total mass of aerosol particles captured on the fiber divided by the total mass of particles passing through the corresponding projected area of the fiber. (Subscripts "D", "I" and "M" denote "convective diffusion", "interception" and "dust load", respectively). The average total mass of particles that have passed through the corresponding projected area of effective fiber length Z_3 between the M^{th} and the $(M + 1)$ -st captures on the effective fiber length of a sample is

$$W_M = \frac{1}{L} \sum_{i=1}^L W_{M,i} / (Z_{\text{tot}} H / Z_3) \quad (6.6.1)$$

where $W_{M,i}$ is the total mass of incoming particles generated on the entire generation plane (dimensionless length Z_{tot} \times dimensionless height $2H$) between the M^{th} and the $(M + 1)$ -st captures on fiber section III of Monte Carlo sample number i , L is the total number of samples, Z_3 is the dimensionless length of fiber section III, H is one half height of the

generation plane, and $Z_{\text{tot}} = Z_1 + Z_2 + Z_3 + Z_4 + Z_5$ is the entire length of the generation plane, which was used in order to minimize end effects.

Then η_{DIM} is simply

$$\eta_{\text{DIM}} = \frac{w_M}{W_M} \quad (6.6.2)$$

where w_M is the average mass of captured particle no M on the effective

length, i.e., $w_M = \frac{1}{L} \sum_{i=1}^L w_{M,i}$.

On the otherhand, the accumulated mass of particles deposited in a unit volume of the filter bed of interest is

$$m = \frac{\alpha w_{\text{cap}}}{\pi Z_3 R_f^3} \quad (6.6.3)$$

where $w_{\text{cap}} = \sum_{M=1}^M w_M$ is the accumulated mass of particles captured on fiber section III, α is the packing density, and R_f is the actual fiber radius (μm).

The single-fiber collection efficiency η_{DIM} of equation (6.6.2) was next normalized with the corresponding Fuch's (1966) clean fiber efficiency η_{DI} , which should correspond to η_{DIO} . The relationship between $\eta_{\text{DIM}}/\eta_{\text{DI}}$ and dust load m is shown for various filtration conditions in Chapter 7. In addition, the single-fiber collection efficiency η_{DIM} was also normalized by η_{DIO} , the efficiency of the first capture. The relationship of $\eta_{\text{DIM}}/\eta_{\text{DI}}$ versus dust load m , and $\eta_{\text{DIM}}/\eta_{\text{DIO}}$ versus dust load m , were expressed in the functional forms

$$\eta_{\text{DIM}}/\eta_{\text{DI}} = 1 + am^b$$

$$\eta_{\text{DIM}}/\eta_{\text{DIO}} = 1 + a'm^{b'}$$
(6.6.4)

by finding the optimum values of a , b , a' and b' such that the sum of squares of differences were minimized. Since the curves were only slightly bended, they could be approximated quite well by the linear functions,

$$\eta_{DIM}/\eta_{DI} = 1 + \lambda m \quad (6.6.5)$$

$$\eta_{DIM}/\eta_{DIO} = 1 + \lambda' m$$

where λ and λ' is the so-called collection efficiency raising factor (Kanoaka et al. 1980).

6.7 Size Distribution of Deposited Particles

In this study the size distribution of incoming aerosol particles was log-normal. It was, therefore, interesting to find out whether the size distribution of deposited particles was also log-normal.

The log-normal distribution is uniquely determined by two constants or parameters. One is the geometric mean d_{pm} , which locates the center of the distribution. The other is the geometric standard deviation σ_g , which measures the spread or variation of individual measurements. The log-normal distribution derives its name from the fact that if the distribution is replotted against $\ln d_p$ or $\log d_p$ instead of the origin d_p , then the resulting distribution will be a normal or Gaussian distribution.

The percentage frequencies beyond $\pm 3 \ln \sigma_g$ are negligibly small. Theoretically, the frequency of occurrences never vanishes entirely, but it rapidly approaches zero as $\ln d_p$ increase. The concentration of values close to $\ln d_{pm}$ is emphasized by the fact that over 2/3 of the observations

lie in the interval $\ln d_{pm} \pm \ln \sigma_g$, while some 95% of them are in the interval $\ln d_{pm} \pm 2 \ln \sigma_g$. Beyond $\pm 3 \ln \sigma_g$ lies only 0.26% of the total frequency.

In this work, the practical range of $6 \ln \sigma_g$ was divided into 30 equal sub-intervals about $\ln d_{pm}$. A deposited particle whose $\ln d_p$ falls into sub-interval i ($i = 1, 2, 3, \dots$) is counted accordingly. In this way, histograms of the sample frequency distribution were prepared for various filtration conditions. The null hypothesis that the size distribution of the deposited particles is log-normal can then be tested using the Chi-square test.